Single-bubble sonoluminescence in sulfuric acid and water: Bubble dynamics, stability, and continuous spectra

Gabriela F. Puente, Pablo García-Martínez, and Fabián J. Bonetto
Laboratorio de Cavitación y Biotecnologia 8400-Instituto Balseiro/Centro Atómico Bariloche-RN-Argentina
(Received 31 July 2005; published 31 January 2007)

We present theoretical calculations of an argon bubble in a liquid solution of 85% wt sulfuric acid and 15% wt water in single-bubble sonoluminescence. We used a model without free parameters to be adjusted. We predict from first principles the region in parameter space for stable bubble evolution, the temporal evolution of the bubble radius, the maximum temperature, pressures, and the light spectra due to thermal emissions. We also used a partial differential equation based model (hydrocode) to compute the temperature and pressure evolutions at the center of the bubble during maximum compression. We found the behavior of this liquid mixture to be very different from water in several aspects. Most of the models in sonoluminescence were compared with water experimental results.

DOI: 10.1103/PhysRevE.75.016314 PACS number(s): 78.60.Mq

Flannigan and Suslick [1] have recently measured the existence of plasma in a sonoluminescent bubble. They used an 85% wt sulfuric acid (H_2SO_4) and 15% wt water mixture as the liquid inside a spherical resonator. The gases dissolved in the liquid mixture were argon, xenon, and neon.

In this work we compute all the relevant characteristics of the system (thermal, fluid, and chemical) as well as the spectra that should be expected from our temperature calculations. All the calculations are performed for an argon bubble in a liquid solution of 85% wt sulfuric acid and 15% wt water.

We outline first the different components of our model. Details of the model are given in [2,3]. The dynamics of the bubble are described by the Rayleigh-Plesset equation [4–6] generalized for nonequilibrium condensation/evaporation mass transfer at the bubble interface [7]. See the reviews by Brenner *et al.* [8] and Barber *et al.* [9] for more details. The ultrasonic pressure in the Rayleigh-Plesset equation is:

$$p_s(t) = P_a \cdot \sin(wt - \phi)$$

where P_a is the ultrasound wave amplitude, w is the angular frequency ($2\pi f = w$), and ϕ is the phase (equal to π).

We compute the transient and spatially nonuniform heat transfer inside the bubble using a collocation point method [10] for low acoustic pressures ($P_a \leqslant 1.2$ bar). For acoustic pressures higher than 1.2 bar the thermal boundary layer is small enough that it can be approximated by one collocation point [11].

We also used the collocation point method to solve the energy equation in the liquid for low acoustic pressures ($P_a \leqslant 1.2$ bar) and a boundary layer approach for acoustic pressures larger than $P_a \approx 1.2$ bar.

We computed the gas diffusion in the liquid and inside the bubble following a similar approach to the one used for the thermal equation obtaining the points in phase space that are stable from a mass diffusive point of view [12].

Nonequilibrium condensation/evaporation is taken into account through the accommodation coefficient [7]. The value for water is taken following the suggestions in [2] to be equal to 0.21. We assume that the amount of sulfuric vapor present in the bubble is negligible at all times.

We took into account water vapor chemical reactions that are important during bubble collapse and chemical reactions of reacting gases dissolved in the liquid mixture [13].

Due to the low water vapor pressure there is very little water vapor inside the bubble during collapse. Therefore argon makes up for almost all of the bubble contents. Having a noble gas as the major constituent allows the upscaling of the sonoluminescence temperatures with minimal endothermic reactions due to the vapors and noncondensable gases. Due to the relatively high temperatures achieved in our calculations we used plasma-type equation of state for the argon [14].

We computed nonuniform temperature and pressure distribution during the few nanoseconds surrounding the bubble collapse to analyze the possible existence of shock waves. Although we computed high temperatures and pressures with a very short duration and weak ionization of the argon gas we did not observe the presence of shock waves in our calculations. We performed these calculations using the hyperbolic partial differential equation (PDE) solver Clawpack. For all calculations the system temperature and pressure are taken to be atmospheric ($P = 10^5$ Pa$=1$ bar and $T = 20\ ^\circ$C$= 293$ K) and the ultrasonic excitation is $P_s(t) = P_a \sin(\omega t - \pi)$ with a frequency $f = 28\,200$ Hz. Table I shows the sulfuric mixture properties we used. where ρ_L is the density, μ_L is the viscosity, c_L is the sound velocity, c_{pL} is the specific heat, k_L is the thermal conductivity, and σ the

TABLE I. SO_4H_2(85% wt)$-H_2O$(15% wt) properties [15].

ρ_L	1778.6 kg/m^3
μ_L	0.015 Pa s
c_L	1473 m/s
c_{pL}	1829.2 J/(kg K)
k_L	0.3578 W/(mK)
σ	0.0712 N/m^2
P_{H2O}	1.00 mbar

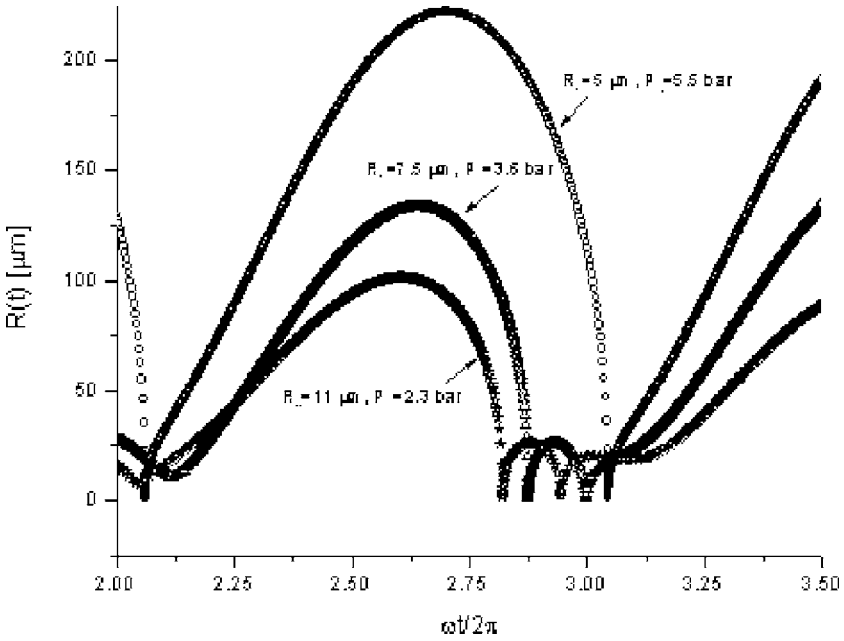

FIG. 1. Temporal evolution of the bubble radius in μm for amplitude acoustic pressures P_a=2.3, 3.6, and 5.5 bars. The ambient radii are chosen to be on the parametric instability boundary.

surface tension of the mixture at 20 °C. p_{H2O} is the vapor pressure.

Figure 1 shows the temporal evolution of the bubble radius for 3 different R_0-P_a combinations. For low acoustic pressures the solution resembles the $R(t)$ for water. As we increase the pressure the expansion phase begins closer to the time of collapse. For high pressures the expansion starts immediately after the time of collapse. For a given P_a the R_0 was chosen as the maximum value compatible with the parametric instability boundary (see Fig. 3).

Figure 2 shows the fixed points in phase space. Figure 2(a) presents the R_0-P_a pairs corresponding to a given concentration $c=c_\infty/c_0$ where c_∞ is the argon concentration in the liquid and c_0 is the saturation concentration of argon in the liquid at room temperature (taken as 20 °C). The c values are small in most of the phase space. We also present the same results in R_0-P_a phase space to a given time of collapse t_c, due to the fact that the experimental determination of t_c is much easier than R_0 [Fig. 2(b)]. From these plots one may conclude that the liquid mixture has to be carefully degassed before the experiment is conducted and that small quantities of argon have to be added to the liquid mixture. The alternative is to use a carrier gas (molecular oxygen or nitrogen for example) but the cost of doing this is that the dissociation of this carrier will be endothermic and the addition will reduce the maximum temperatures.

We computed the shape instability threshold ([16,12]) for bubbles with imposed concentrations instead of considering the ambient radius known. In a particular experiment the gas concentration is fixed. The experimenter controls also the acoustic pressure intensity but not the ambient radius. We present the results the usual way (i.e., P_a and R_0 are independent variables and c is a result of the calculation). But the control parameters of the experiment are P_0 and c. We called this "imposed concentration." We included the effect of the viscosity in our analysis but not the effect of vorticity [10]. We also computed the instability due to the Bjerknes force [17] and the Rayleigh-Taylor instability [18].

Figures 3(a)–3(c) shows the stability region for bubbles in the R_0-P_a phase space for the parametric instability [(PI), Fig. 3(a)], for the Bjerknes force instability [(BI), Fig. 3(b)], and for the Rayleigh-Taylor instability [(RTI) Fig. 3(c)].

Figure 3(a) shows that for the region of interest in the phase space a bubble is more likely to be PI stable for low P_a. Also the range of R_0 that corresponds to stable bubbles for a fixed P_a becomes smaller as the P_a is increased. The upper R_0 limit is approximately R_0=27 μm at P_a=1 bar, and R_0=2.4 μm at P_a=4.8 bar.

Figure 3(b) shows that a bubble is Bjerknes force unstable for almost all the phase space under investigation. Only a small triangular region [inset in Fig. 3(b)] for relatively small acoustic pressures ($P_a<1.8$ bar) and for relative small ambient radius ($R_0<1.4$ μm) is stable. In the unstable region a bubble undergoing oscillations at the center of the resonator will experiment a net force that takes the bubble away from the center. When we compare this behavior with the behavior observed in water we find it to be very different. In water the bubble is lost (extinction) for acoustic pressures that are smaller than the ones corresponding to an unstable BI. The fact that the bubble is unstable for the BI explains why it is very difficult to produce a stationary bubble at the center of the resonator with sulfuric acid (aq.).

A very significant difference between the results presented in Figs. 3(a)–3(c) and the corresponding margin stability boundary for pure water is with respect to the Rayleigh-Taylor instability. Akhatov *et al.* [17] found that in water a bubble with R_0=4 μm became unstable for an acoustic pressure of P_a=1.78 bar. Augsdörfer *et al.* [18] computed the R-T instability threshold for water and found that with R_0=4 μm the bubble became unstable for an acoustic pressure of P_a=1.25 bar. Augsdörfer *et al.* [18] also computed the parametric instability threshold obtaining P_a=1.5 bar for R_0=4 μm. These results suggest that the R-T instability is the cause for the bubble disappearance in water. For a fixed R_0 a bubble in pure water encounters the Rayleigh-Taylor instability for the lowest acoustic pressure P_a compared to

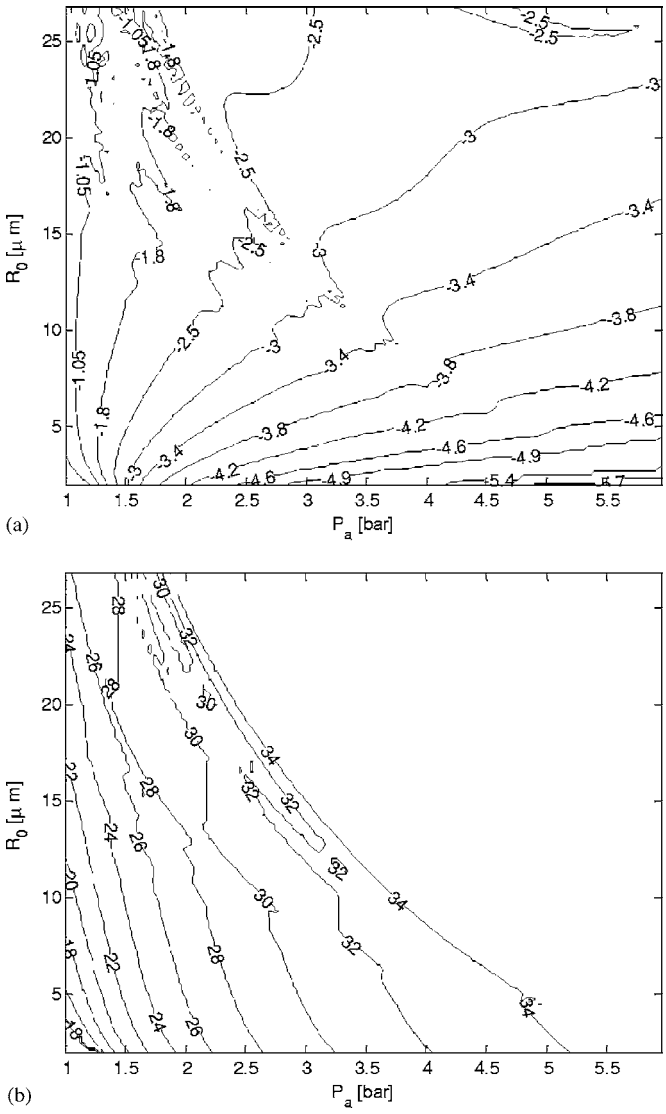

FIG. 2. (a) Fixed points of the model. The plot shows the relationship between the ambient radius R_0 as a function of P_a and $\log_{10}(c)$. For each point (R_0, P_a) we computed the corresponding nondimensional concentration c value. The curves are log spaced for clarity. (b) Fixed points of the model. The time of collapse t_c in microseconds is plotted as a function of R_0 and P_a. The time of collapse t_c is the time interval between the moment when the acoustic pressure is zero with negative slope and the moment of maximum bubble collapse.

the other types of instability. In sulfuric acid Fig. 3(c) shows that a bubble with a $R_0=4$ μm and $P_a=5$ bar is RT stable.

The RT stability boundary for sulfuric for a given R_0 is present at a much higher P_a than the water value. We believe that this is the main reason why high acoustic pressures (and consequently high maximum temperatures) can be achieved with sulfuric acid.

From the results shown in Fig. 3 we cannot see clearly any instability that would produce the bubble extinction. Let us take each type of instability in turn. The parametric instability sets a high limit for the amount of gas in a bubble R_0 for a given acoustic pressure P_a. If the bubble is characterized for a (P_a, R_0) where the bubble grows due to mass dif-

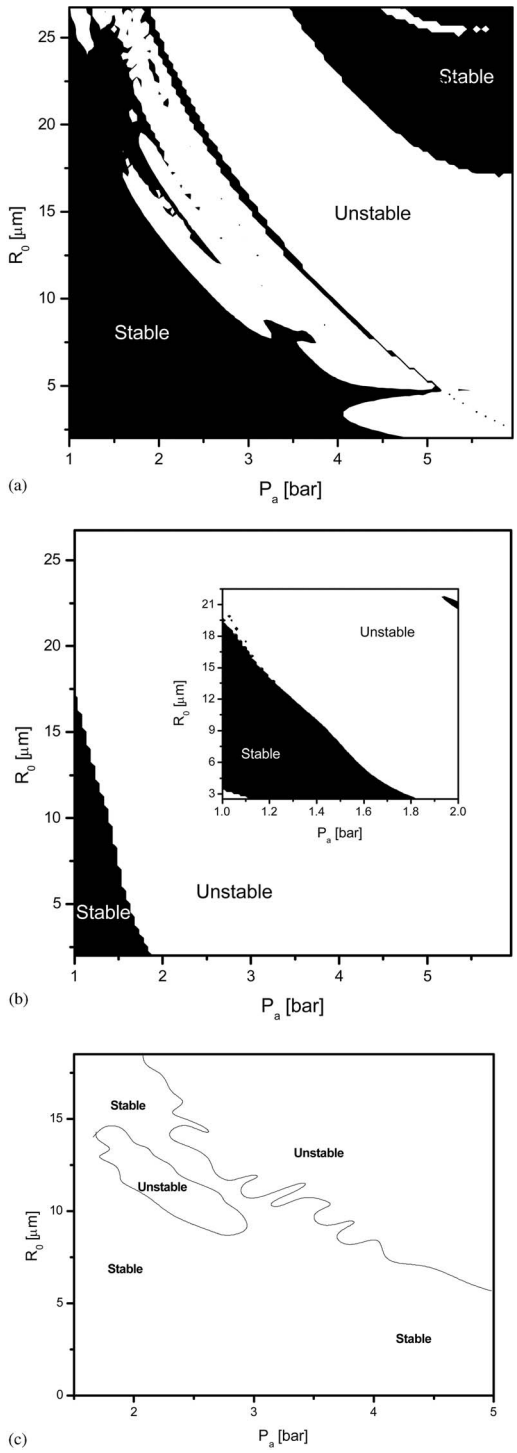

FIG. 3. Phase space diagram of the parametric instability (a), the Bjerknes force instability (b), and the Rayleigh-Taylor instability (c). In (a) and (b) a white color indicates an unstable fixed point. In Fig. 3(c) the main trend of the PI threshold is also shown together with the RT instability. In Fig. 3(c) two RT curves are presented. For 3 bar$<P_a<$5.5 bar a fixed point is stable if it lies below the single RT curve. For 2 bar$<P_a<$3 bar the fix point is stable if it lies below the lower RT curve and unstable if it lies above the upper curve. In the latter range there is a third curve (not shown for clarity).

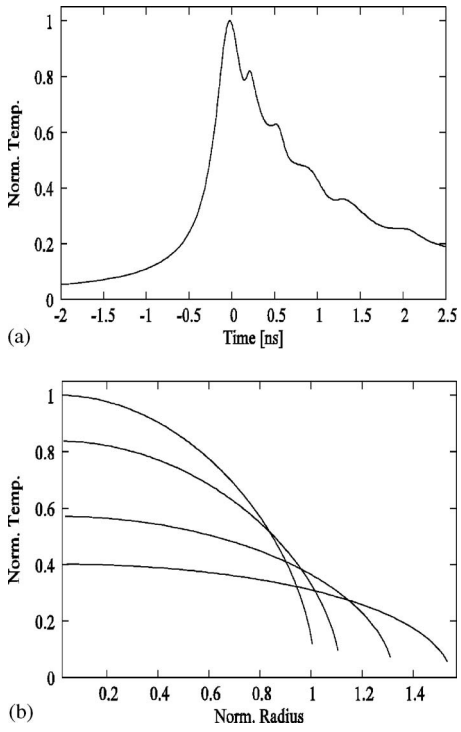

FIG. 4. (a): Temporal evolution of the center temperature for the detailed calculation (PDE). This is a sulfuric acid calculation with $R_0=11$ μm, $P_a=2.3$ bar which corresponds to an argon concentration $c=0.24$. The maximum temperature for the simulation was $T=117\,560$ K at $r=0$ (bubble center) and t approximately 0 (time of collapse). (b): Temporal evolution of the radial distribution of the temperature (every 10 picoseconds before collapse. The normalized temperature T is equal to 1 at the bubble center ($r=0$) location at the time of collapse. The different curves correspond to different times form the time of collapse. This figure corresponds to the detailed calculation (PDE).

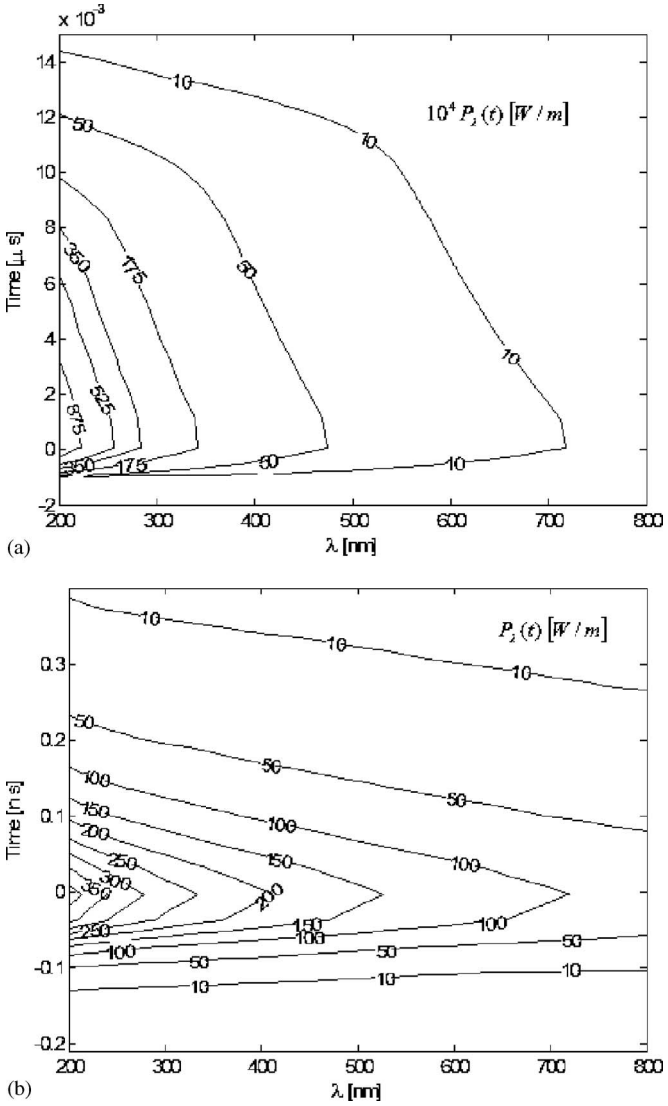

FIG. 5. Time resolved continuous spectra of the emitting bubble for (a) sulfuric acid mixture and (b) water. The parameters for 5(a) are $R_0=5$ μm, $P_a=5.5$ bar. The computed maximum temperature is $T=169\,000$ K and the minimum bubble radius is $R=0.7$ μm. The parameters for (b) are $R_0=4$ μm, $P_a=1.4$ bar which corresponds to an argon concentration $c=0.24$ (which converts to 24% air in water). The maximum temperature is $T=17\,200$ K and the minimum bubble radius is $R=0.7$ μm. The parameters used in water are close to bubble extinction condition. Note that the scale in the sulfuric acid plot is four orders of magnitude compared to water. The computed light fluence in sulfuric is three orders of magnitude higher than the fluence in water. Time equal to 0 corresponds to time of minimum radius.

fusion a mechanism must exist to eject mass from the bubble and keep it on the PI boundary. This is in fact observed in water experiments. The conclusion is that PI will not produce the bubble extinction but instead will control the maximum amount of gas in the bubble. The Bjerknes force instability (BI) sets a maximum value for the R_0 for a given acoustic pressure P_a for the bubble to be stable at the resonator center but the bubble may still be off center. Another major difference between an Ar-in-sulfuric bubble and an Ar-in-water bubble is that at a critical acoustic pressure P_a the moving sulfuric bubble goes away from the resonator center.

Figure 4 shows the results of the spatially nonuniform simulation of the bubble collapse. Figure 4(a) shows the temperature evolution of the bubble center. We see that the maximum temperatures are achieved at time very near 0 (defined as the time of the minimum bubble radius).

The temperatures obtained in Fig. 4(a) are enough to produce ionization in the argon atoms. We used the multielectron Saha equation to compute the fraction of argon atoms that are ionized getting a value of the order of 1%. We assumed the electrons resulting from the ionization, the Ar ions and the Ar neutral atoms, to be in equilibrium due to the fact the average time between collisions is of the order of picoseconds. Figure 4(b) shows the radial distribution of the bubble temperature computed with the hyperbolic PDE solver. We can see that no shock waves are present and that the temperature profiles are fairly uniform.

Figure 5 shows the computed time resolved light emitted spectra obtained from the temperature, and number of particles in the bubble [19]. For this discussion when we say temperature we mean maximum temperature at the center. We did not compute the light emitted (mainly in the infrared) due to the excited Ar atoms and measured in [1]. The spatial

uniformity assumption in the temperature allows for closed form solutions for the spectra of the light emitted by the bubble. We did not use the temperature profile information in this computations. The fact that the spectra resembles the spectrum expected for a blackbody radiator at a much lower temperature is due to the fact that the bubble behaves as a volume emitter [19].

Some effects that were not taken into account in the results presented so far are the presence of SO_4H_2 vapor based on the fact that there is much more water vapor in the bubble, the dissociation of these vapors and the spatial nonuniformities in the temperature affecting the spectra of the light emitted by the bubble.

In summary we present in this paper detailed bubble dynamics computations of a H_2SO_4 (aq.) liquid mixture that contains argon gas dissolved in it. They include the bubble radius temporal evolution, the shape instability that ends up in the parametric instability, and the shape instability associated with Rayleigh-Taylor instability. We present the fixed points of the system in phase space. We also present the instability regions in phase space for parametric, Bjerknes force, and Rayleigh-Taylor instabilities. We stress the differences with respect to a water-argon system.

We show detailed (PDE) calculations for a representative condition in phase space. We find that no shock waves are formed during the temporal evolution. Even without the presence of shock waves we find that a fraction of the argon atoms are ionized during a short period of time. Finally we present time resolved spectra for both sulfuric acid and water.

The picture that emerges from the analysis of these dynamic data is that the main cause for the differences between the sulfuric acid behavior and the water behavior is that in sulfuric the RT instability occurs at acoustic pressures that are much higher than in water. The Bjerknes force may move the bubble in sulfuric away from the resonator center but it does not seem to be capable of producing the bubble extinction. The parametric instability controls the maximum ambient radius compatible with a given acoustic pressure but it does not produce bubble extinction. In water on the other hand RT acts at acoustic pressures of the order of 1.4 bar producing the bubble extinction.

The picture that emerges from the temperature and spectra calculations is that the temperatures obtained in the sulfuric calculations are enough to justify the presence of Ar ions and the 1000-fold increase in the light emission when compared to water.

For helpful discussions we thank Raúl Urteaga and Damián Dellavale. G.F.P. was financed by Anpcyt/Secyt. The partial support of Foncyt/Anpcyt/Secyt through Grant No. PICT 12-09848 is gratefully appreciated.

[1] D. J. Flannigan and K. S. Suslick, Nature (London) **434**, 52 (2005).
[2] G. F. Puente and F. J. Bonetto, Phys. Rev. E **71**, 056309 (2005).
[3] G. F. Puente, R. Urteaga, and F. J. Bonetto, Phys. Rev. E **72**, 046305 (2005).
[4] L. Rayleigh, Philos. Mag. **34**, 94 (1917).
[5] M. Plesset, J. Appl. Mech. **16**, 277 (1949).
[6] R. Toegel and D. Lohse, J. Chem. Phys. **118**, 1863 (2003).
[7] K. Yasui, J. Phys. Soc. Jpn. **66**, 2911 (1997).
[8] M. Brenner, S. Hilgenfeldt, and D. Lohse, Rev. Mod. Phys. **74**, 425 (2002).
[9] B. P. Barber and S. J. Putterman, Phys. Rev. Lett. **69**, 3839 (1992).
[10] Y. Hao and A. Prosperetti, Phys. Fluids **11**, 1309 (1999).
[11] R. Toegel, B. Gompf, R. Pecha, and D. Lohse, Phys. Rev. Lett. **85**, 3165 (2000).
[12] S. Hilgenfeldt, D. Lohse, and M. Brenner, Phys. Fluids **8**, 2808 (1996).
[13] V. Kamath, A. Prosperetti, and F. Egolfopoulos, J. Acoust. Soc. Am. **94**, 248 (1993).
[14] B. D. Storey and A. J. Szeri, Proc. R. Soc. London, Ser. A **456**, 1685 (2000).
[15] *Handbook of Chemistry and Physics*, 48th edition, edited by R. Weast (CRC Press, Boca Raton, FL, 1968).
[16] A. Eller and L. A. Crum, J. Acoust. Soc. Am. **47**, 772 (1970).
[17] I. Akhatov, R. Mettin, C. D. Ohl, U. Parlitz, and W. Lauterborn, Phys. Rev. E **55**, 3747 (1997).
[18] U. H. Augsdorfer, A. K. Evans, and D. P. Oxley, Phys. Rev. E **61**, 5278 (2000).
[19] S. Hilgenfeldt, S. Grossman, and D. Lohse, Phys. Fluids **11**, 1318 (1999).